

## Microstructure evolution of a new directionally solidified Ni-based superalloy after long-term aging at 950 °C upto 1 000 h

HUANG Yan<sup>1</sup>, WANG Lei<sup>1</sup>, LIU Yang<sup>1</sup>, FU Shun-ming<sup>1</sup>, WU Jian-tao<sup>2</sup>, YAN Ping<sup>2</sup>

1. Key Laboratory for Anisotropy and Texture of Materials, Northeastern University, Shenyang 110819, China;

2. Department of High-temperature Materials, Central Iron and Steel Research Institute, Beijing 100081, China

Received 30 October 2010; accepted 27 May 2011

**Abstract:** The microstructure evolution of a new directionally solidified (DS) Ni-based superalloy used for gas turbine blades after long-term aging at 950 °C was investigated. The results show that the  $\gamma'$  phase becomes more regular in dendritic arm and interdendritic area, while both the mass fraction and the size of  $\gamma'$  phase increase gradually with increasing aging time. During long-term aging, the MC carbide dissolves on the edge to provide the carbon for the formation of  $M_{23}C_6$  carbide by the precipitation of Cr at the grain boundary. The rose-shaped  $\gamma'/\gamma$  eutectic partly dissolves into  $\gamma$  matrix and the aging promotes it transform into raft-shape  $\gamma'$ . The microstructure is generally stable and no needle-like topologically close-packed phase (TCP) can be found after aging for 1 000 h.

**Key words:** Ni-based superalloy; long-term aging; microstructures evolution; carbides;  $\gamma'$  phase

### 1 Introduction

The directionally solidified (DS) Ni-based superalloy possesses good physical, mechanical and corrosion properties and high stability at high temperatures, so it has been widely used as parts in fields of aviation and aerospace [1–3]. Due to the elimination of grain boundaries and the introduction of a preferred grain orientation by DS casting [4], it becomes the first choice materials to apply for advanced gas turbine blades. During service, the alloy used as gas turbine blades is subjected to severe working conditions, such as high temperature and long time. As a result, the microstructure of the alloy greatly changes [5]. However, all the properties of the alloy are dependent on microstructure. Therefore, the microstructural stability of the superalloy is a critical issue for the reliability and economy of entire gas turbine systems [6–8]. In recent years, more researchers focused on the microstructure evolution and the degeneration of microstructure during long-term aging at high temperature for safety in utilization [9–10]. They summarized some rules of microstructure in the superalloy after long-term aging, such as coarsening of  $\gamma'$  phase [11], decomposition of

prime carbide [12–13] and precipitation of second phase [14]. In the present work, the microstructural stability of the new Ni-based superalloy developed by directionally solidified (DS) technology at 950 °C for 1 000 h used as the gas turbine blades was investigated. The complex and multi-phase microstructures of the alloy were studied. The microstructure evolution process of the alloy was also summarized.

### 2 Experimental

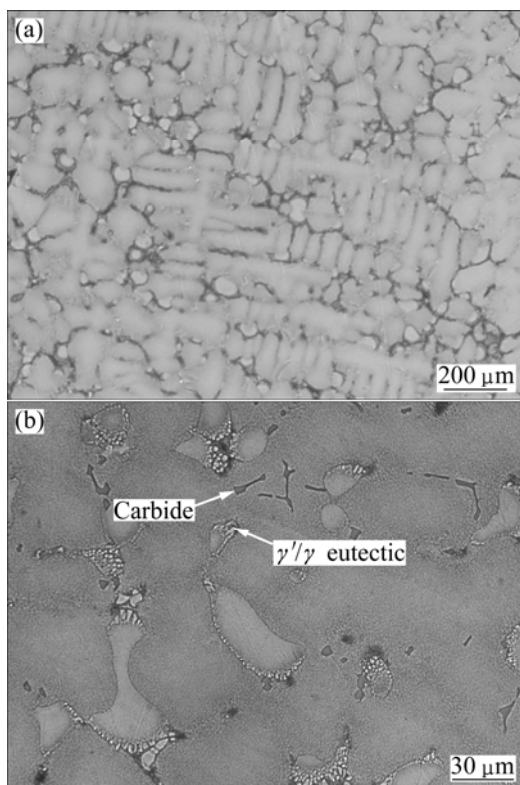
A new directionally solidified Ni-based superalloy with the chemical composition (mass fraction, %) of 0.12 C, 12.3 Cr, 8.9 Co, 4.4 W, 1.8 Mo, 4.0 Ta, 3.4 Al, 3.9 Ti, 1.0 Hf, 0.014 B, 0.05 Zr and balance Ni was used in the present research. The alloy was prepared by double vacuum method and directionally cast into the bar with dimensions of  $d13 \text{ mm} \times 220 \text{ mm}$ . Then, the samples were sectioned into 10 mm in height for preparation of metallographic samples and subsequent long-term aging treatment. The samples were standard heat-treated at 1 180 °C for 2 h followed by air cooling, and then held at 845 °C for 24 h with air cooling. After standard heat-treatment, the samples were subjected to long-term aging for 100, 500 and 1 000 h at 950 °C, respectively.

The microstructures of samples aged at each stage were examined by an optical microscope (OLYMPUS GX71 type) and a laser scanning confocal microscope (OLYMPUS OLS 3100 type), as well as the field emission scanning electron microscope (JEOL 7001 type) with an energy dispersive spectroscope (EDS). The specimens for observation were etched in a solution consisting of 4 g CuSO<sub>4</sub>, 20 mL HCl and 80 mL C<sub>2</sub>H<sub>5</sub>OH. High magnification observation was carried out on a transmission electron microscope (TECNAL G2 20) and the thin foil was electropolished with an electrolyte consisting of 10% HClO<sub>4</sub> and 90% C<sub>2</sub>H<sub>5</sub>OH at -25 °C.

### 3 Results and discussion

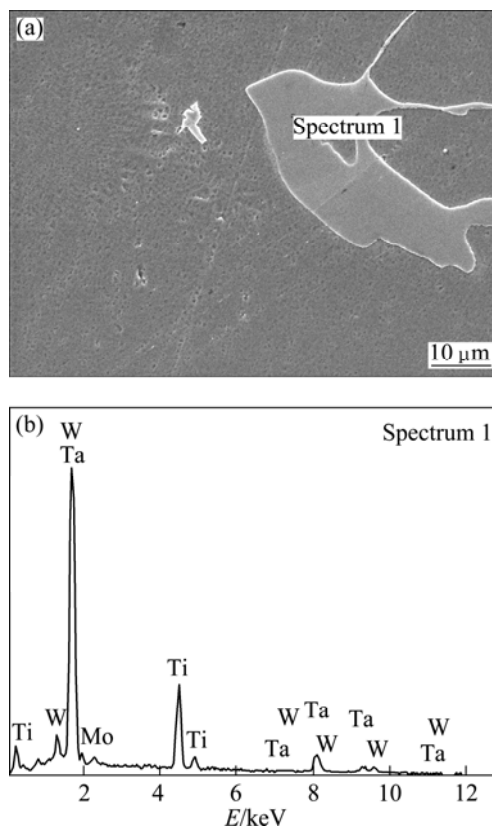
#### 3.1 Microstructure characteristics of as-cast alloy

Figure 1 shows the microstructure of the as-cast samples. The dendrite and interdendrite region in the as-cast alloy can be seen clearly. The microstructure of the alloy is composed of  $\gamma'/\gamma$  eutectic,  $\gamma'$  phase,  $\gamma$  matrix and carbides. The rose-shaped  $\gamma'/\gamma$  eutectics are distributed in interdendritic area, which is the last solidified part. The carbides are observed in the interdendritic area with both block shape and rod shape, as shown in Fig. 1(b). According to EDS pattern shown in Fig. 2, the carbide is rich in Ta (41.02% in mass fraction) and Ti (50.91%), probably TaC and TiC, which



**Fig. 1** Optical micrographs of as-cast alloy: (a) Dendritic pattern; (b)  $\gamma'/\gamma$  eutectic and carbide

is similar to other superalloy. MC carbides with the high carbon contents among the other kinds of carbides are the resources of the carbon for the formation of other carbides in the subsequent heat treatments or services. Through SEM observation shown in Fig. 3, it is clear that the primary  $\gamma'$  is of cubic type with a diameter of 0.2–0.6  $\mu\text{m}$ .



**Fig. 2** SEM image (a) and EDS spectrum (b) of MC carbide of as-cast alloy

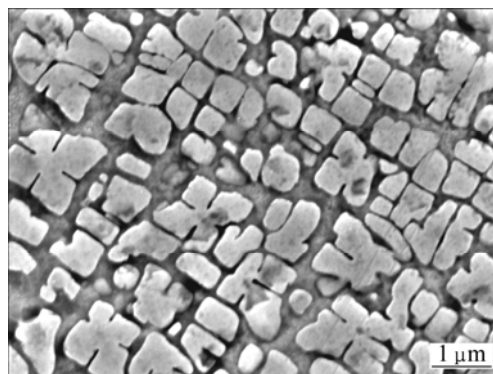


**Fig. 3** SEM image of  $\gamma'$  phase in as-cast alloy

#### 3.2 Microstructure characteristics of alloy after aging

Figure 4 shows the OM photographs of  $\gamma'$  phases in alloys aged for different time. It can be found that the morphology of  $\gamma'$  phases is near spherical, and their size is almost the same. With increasing aging time, the  $\gamma'$  phase grows gradually. Heavy elements such as W and

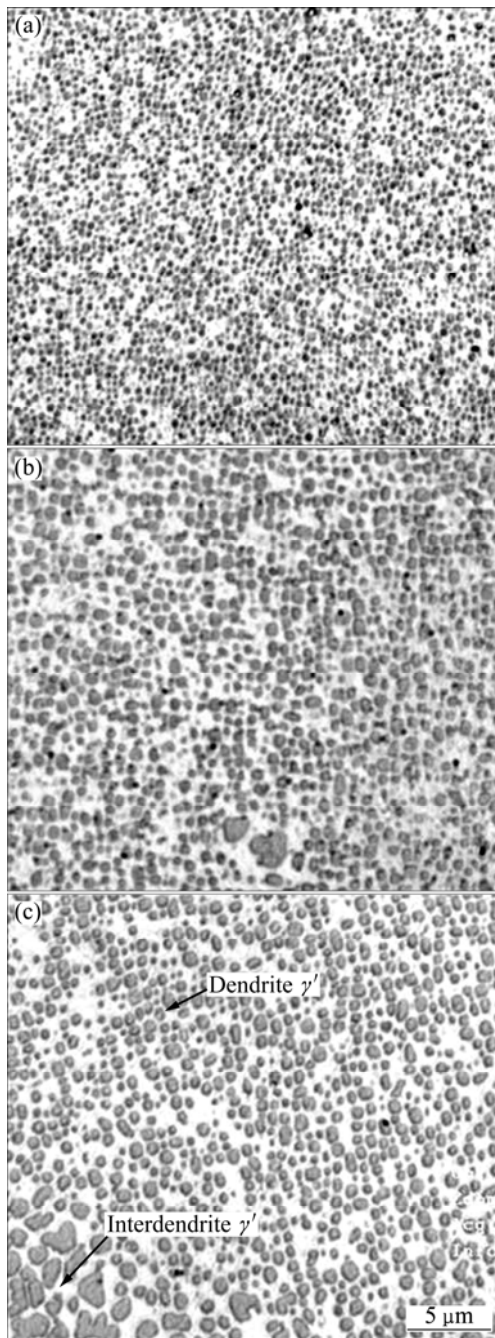


**Fig. 4** Optical micrographs of  $\gamma'$  phase in alloys aged at 950 °C for 100 h (a), 500 h (b) and 1 000 h (c)

Mo with high melting points tend to segregate at the core of dendrites, while the interdendrite region of microstructure enriches in Al and Ti [15]. Therefore, the average size of  $\gamma'$  phase in the interdendrite regions is larger than that in the dendrite cores, as shown in Fig. 4(c), but the  $\gamma'$  phase in interdendrite regions has an irregular cubic morphology. At the same time,  $\gamma'$  phase remains cuboidal under whole testing conditions, and there is no particle agglomeration in the dendrite region, as shown in the Fig. 5. The  $\gamma'$  coarsening during the long-term aging follows Wagner's theory of Oswald

maturing to  $\gamma'$ , which is realized by the dissolution of small  $\gamma'$  and the growing of big  $\gamma'$ . When a moving dislocation encounters a series of obstacles, the obstacles will hinder the moving of dislocation. With the growing of  $\gamma'$ , the distance between two neighbor  $\gamma'$  phase increases. When a dislocation passes large obstacles, there will be a dislocation loop left behind the obstacles, and the resistance for dislocation to move decreases. Thus, the strengthening effect is smaller. Therefore, with the increase of aging time, the  $\gamma'$  phases grow gradually, resulting in the decrease of strength.

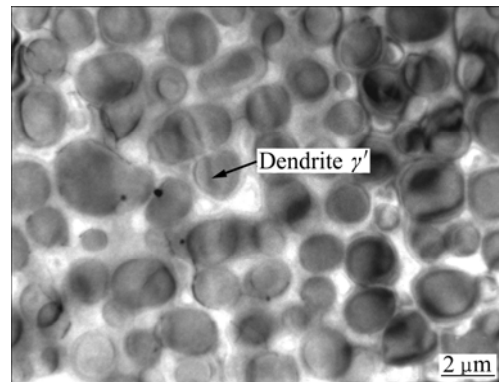


**Fig. 5** TEM image of  $\gamma'$  phase in alloy aged at 950 °C for 1 000 h

There are mainly two kinds of carbides in this alloy after long-term aging, which are MC and  $M_{23}C_6$ . MC carbides are prime carbides, which can be easily observed with plates and regular geometric shape. During aging, the carbide morphology changes slightly, as shown in Fig. 6, which shows that the carbides dissolve on the edge during aging, and this variation starts from aging of 100 h, and becomes obvious with increasing the aging time. According to the EDS analyses (Table 1), it is found that no change occurs in the composition of carbides after long-term aging, as shown in Fig. 7 (remarked with A). While, the dissolution part of carbides, as shown in Fig. 7 (remarked with B), is rich in Al, Ti and Ni which almost have become a part of the matrix.

On the other hand, after aging the grain boundary carbides  $M_{23}C_6$  (as shown in Fig. 8) can be seen, which cannot be found under the as-cast condition. During the aging at 950 °C, MC carbide changes into the  $M_{23}C_6$  grain boundary carbides. By the EDS analysis of the carbide at grain boundary, it is found that the carbides are rich in Cr. After aging for a relatively long time, MC type carbide reacts with the matrix by  $MC + \gamma \rightarrow M_{23}C_6 + \gamma'$  [16]. As shown in Fig. 8, the  $M_{23}C_6$  type carbides are distributed at the grain boundary, and their size becomes larger with increasing the aging time. When carbides are granular, the strengthening mechanism is the same as

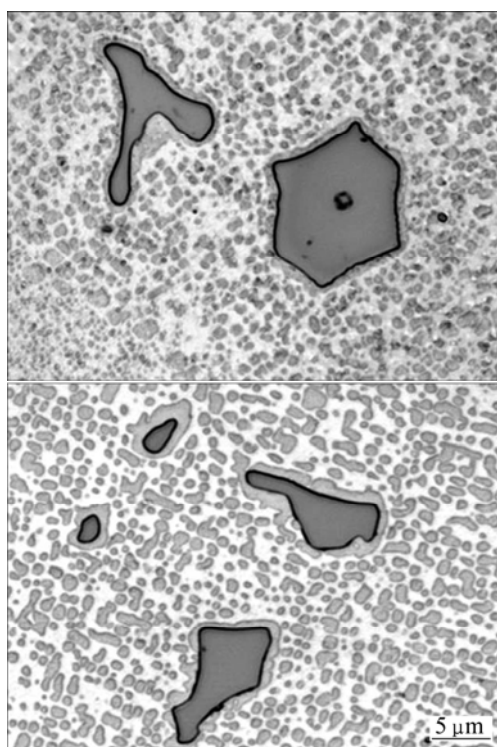


**Fig. 6** Optical micrographs of dissolved carbides in alloys aged at 950 °C for 100 h (a) and 500 h (b)

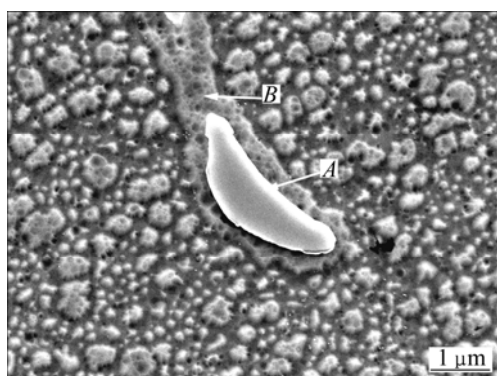


**Fig. 7** SEM image of dissolved carbides in alloy aged at 950 °C for 1 000 h

**Table 1** EDS point analysis results of chemical compositions

Element	Point A in Fig. 7		Point B in Fig. 7	
	w/%	x/%	w/%	x/%
Ti	19.90	45.20	5.79	7.09
Cr	0.75	1.57	3.27	3.69
Ni	3.20	5.93	68.75	68.71
Mo	3.00	3.41	6.01	5.99
Hf	2.90	1.77	5.03	10.93
Ta	60.00	36.07	6.61	2.14
W	10.24	6.06	4.54	1.45

that of  $\gamma'$  precipitate. So, it is helpful that the block carbides dissolve into small carbides after the aging. Nevertheless, when the alloy is aged for a long time, the

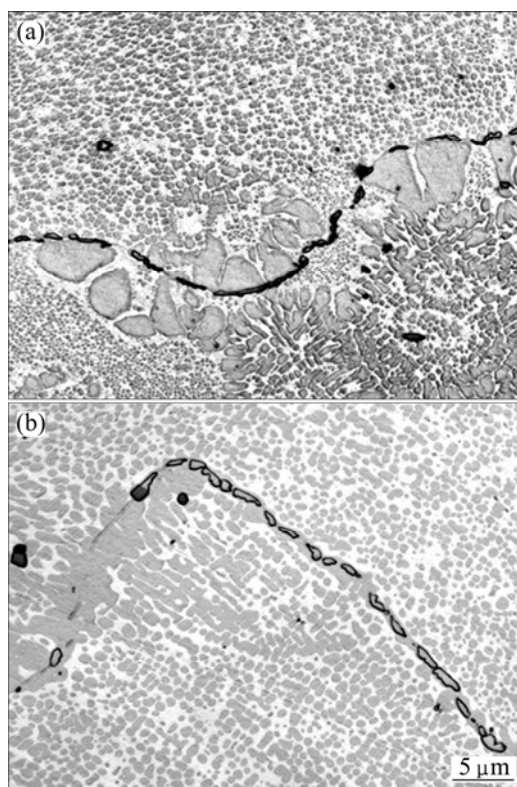


**Fig. 8** Optical micrographs of grain boundary carbides in alloys aged at 950 °C for 100 h (a) and 1 000 h (b)

precipitated carbides along grain boundary connect with each other and the sizes of grain boundary carbides increase. These grains are encompassed by these chain-like carbides, and crack may be formed easily. Because of above reasons, chain-like carbides along grain boundary are detrimental, and can decrease the strength and other mechanical properties of the alloy. As well known, the plasticity of carbides is lower than that of the matrix, since the carbides can be enlarged after long-term aging, which will be very helpful for the plasticity of the alloy. However, it is important to avoid the carbides to continuously distribute at the grain boundary, so that it will cause the grain boundary brittleness.

The  $\gamma'/\gamma$  eutectic is an indication of the remaining melt at the end of the solidification process. After solution heat treatment at 1 180 °C for 2 h, the microstructure with  $\gamma'/\gamma$  eutectic has been homogenized and alloying element segregation become weaker and weaker, while the primary  $\gamma'$  in the as-cast alloy cannot be resolved fully. Figure 9 shows that the  $\gamma'/\gamma$  eutectic like rose remains during the aging. It can be noticed that with increasing the aging time, the  $\gamma'/\gamma$  eutectic partly dissolves into  $\gamma$  matrix, at the same time, the shape of  $\gamma'$  changes into the shape of raft, but the chemical composition of  $\gamma'/\gamma$  eutectic changes a little after aging under the experimental conditions.

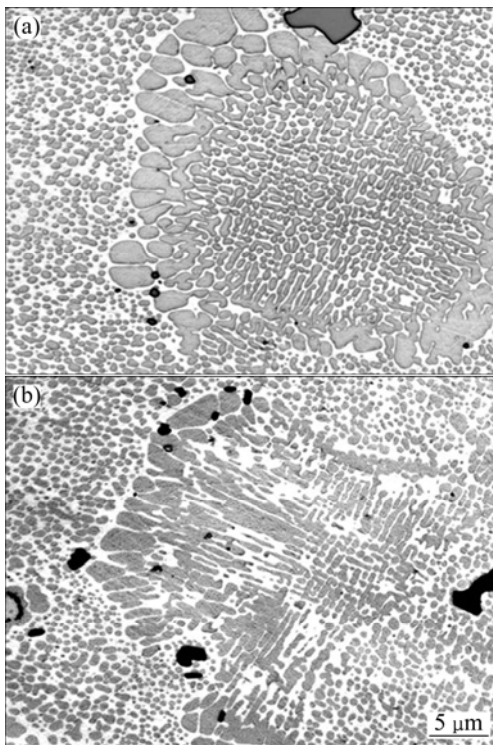


**Fig. 9** Optical micrographs of  $\gamma/\gamma'$  eutectics in alloys aged at 950 °C for 100 h (a) and 500 h (b)

Figure 10 shows the optical micrograph of the alloy after aging for 1 000 h. Due to the element diffusion, the distribution of alloying elements in the alloy tends to be more homogeneous. The difference between the interdendrite and dendrite becomes vaguer and vaguer. And no needle-like TCP affecting the mechanical properties of the alloy can be found after aging for 1 000 h. Based on the results, it can be considered that the microstructure of new directionally solidified alloy is generally stable at 950 °C.

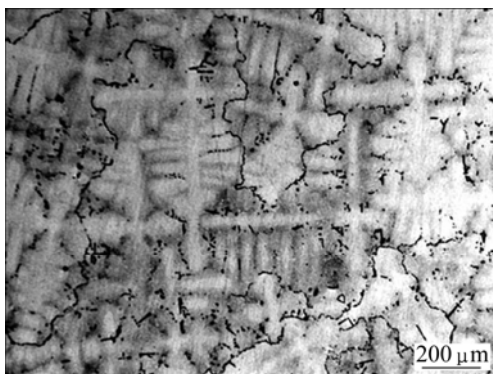


**Fig. 10** Optical micrograph of alloy aged at 950 °C for 1 000 h

## 4 Conclusions

1) The microstructure of the as-cast alloy was composed of coarse  $\gamma'$  precipitates, hyperfine  $\gamma'$  particles in the matrix,  $\gamma'/\gamma$  eutectic and blocky carbides.

2) With increasing the aging time, the  $\gamma'$  phases in both dendritic and interdendritic grew and changed from spherical into cubic morphology.

3) During aging, part of MC type carbides reacted with the matrix and changed into  $M_{23}C_6$  type carbides.

4) After long-term aging, the  $\gamma'/\gamma$  eutectic partly dissolved into  $\gamma$  matrix, and at the same time, the shape of  $\gamma'$  changed into the shape of raft.

## References

- [1] GUO Jian-ting. Materials science and engineering for superalloys [M]. Beijing: Science Press, 2008. (in Chinese)
- [2] SUN Lian, ZOU Jin-wen. Research and development of disc PM superalloy [J]. Aviation Engineering and Maintenance, 2001(1): 28–30. (in Chinese)
- [3] ZHANG Jian, SINGER R F. Hot tearing of nickel-based superalloys during directional solidification [J]. Acta Materialia, 2002, 50: 1869–1879.
- [4] ZHOU Yi-zhou, VOLEK A, SINGER R F. Influence of solidification conditions on the castability of nickel-base superalloy IN792 [J]. Metallurgical and Materials Transaction A, 2005, 36: 651–656.
- [5] YANG Jia-xia, ZHENG Qi, ZHANG Hong-yu, SUN Xiao-feng, GUAN Heng-rong, HU Zhuang-qi. Effects of heat treatments on the microstructure of IN792 alloy [J]. Materials Science and Engineering A, 2010, 527: 1016–1021.
- [6] SRINIWASAN D. Effect of long-time exposure on the evolution of minor phases in alloy 718 [J]. Materials Science and Engineering A, 2004, 364: 27–34.
- [7] LIU Jiang-wen, JIAO Dang-ling, LUO Cheng-ping. Microstructural evolution in austenitic heat-resistant cast steel 35Cr25Ni12NbRE during long-term service [J]. Materials Science and Engineering A, 2010, 527: 2772–2779.
- [8] GUO Wei-min, WU Jian-tao, ZHANG Feng-ge, ZHAO Ming-han. Microstructure properties and heat treatment process of powder metallurgy superalloy FGH95 [J]. Journal of Iron and Steel Research, 2006, 13(5): 65–68. (in Chinese)
- [9] SAJJADI S A, ZEBARJAD S M, GUTHRIE R I L, ISAC M. Microstructure evolution of high-performance Ni-base superalloy GTD-111 with heat treatment parameters [J]. Journal of Materials Processing Technology, 2006, 175: 376–381.
- [10] SAFARI J, NATEGH S. On the heat treatment of Rene-80 nickel-base superalloy [J]. Journal of Materials Processing Technology, 2006, 176: 240–250.
- [11] GUAN Xia-rong, LIU En-ze, LIU Feng, ZHENG Zhi, TONG Jian, ZHAI Yu-chun. Effects of Ti on  $\gamma'$  phase in aging structure of Ni-based superalloy [J]. Non Ferrous and Metallurgy, 2010, 26(6): 32–36. (in Chinese)
- [12] MA Xiao-fen, LIU En-ze, GUAN Xiu-rong, ZHENG Zhi, TONG Jian, NING Li-kun, HUI Sheng. Carbides of a new directional solidification superalloy DZ68 [J]. Heat Treatment of Metals, 2010, 35(4): 10–13. (in Chinese)
- [13] WU Kai, LIU Guo-quan, HU Ben-fu, WU Hao, ZHANG Yi-wen, TAO Yu, LIU Jian-tao. Carbides in a new type Hf-Ta-containing nickel-based superalloy powder [J]. Journal of University of Science and Technology Beijing, 2010, 32(11): 1464–1470. (in Chinese)
- [14] SHI Zhen-xue, LI Jia-rong, LIU Shi-zhong, LUO Yu-shi, ZHAO Jian-qian. Effect of Hf content on the microstructures and stress

- rupture properties of DD6 single crystal superalloy [J]. Rare Metal Materials and Engineering, 2010, 39(8): 1334–1338. (in Chinese)
- [15] LIU Li-rong, JIN Tao, SUN Xiao-feng, GUAN Heng-rong, HU Zhuang-qi. Effect of Al, Ti and Ta contents on the microstructure in Ni-base single crystal superalloy during aging [J]. Rare Metal Materials and Engineering, 2008, 37(7): 1253–1256. (in Chinese)
- [16] ZHENG Liang, XIAO Cheng-bo, TANG Ding-zhong, GU Guo-hong, TANG Xin. Investigation of the solidification behavior of a high Cr content cast Ni-Base superalloy K4648 [J]. Rare Metal Materials and Engineering, 2008, 37(9): 1539–1544. (in Chinese)

## 一种定向凝固镍基高温合金 950 °C 长期时效 1 000 h 的组织演变

黄炎<sup>1</sup>, 王磊<sup>1</sup>, 刘杨<sup>1</sup>, 付顺明<sup>1</sup>, 吴剑涛<sup>2</sup>, 燕平<sup>2</sup>

1. 东北大学 材料各向异性与织构工程教育部重点实验室, 沈阳 110819;
2. 钢铁研究总院 高温材料研究所, 北京 100081

**摘要:** 研究一种用于燃气轮机叶片的定向凝固镍基高温合金在 950 °C 长期时效 1 000 h 后的组织演变。结果表明: 随着时效时间的延长, 在枝晶和枝晶间的  $\gamma'$  相变得更加有规则, 而且  $\gamma'$  相的质量分数和尺寸也随着时效时间的延长而逐渐增加。在时效过程中, MC 型碳化物的边缘部分发生溶解, 而由其提供的碳元素与析出的 Cr 元素在晶界处形成  $M_{23}C_6$  型碳化物。玫瑰状的  $\gamma'/\gamma$  共晶部分溶解进入基体, 时效过程也促进其向筏形  $\gamma'$  转变。合金经过 1 000 h 时效后, 结构总体上是稳定的, 没有发现针状的 TCP 相。

**关键词:** 镍基高温合金; 长期时效; 组织演变; 碳化物;  $\gamma'$  相

(Edited by YANG Hua)